ELSEVIER

Experimental study of flash atomization of binary hydrocarbon liquids

T. Gemci [a], K. Yakut [a], N. Chigier [a],*, T.C. Ho [b]

[a] *Spray Systems Technology Center, Carnegie Mellon University, Pittsburgh, PA 15213, USA*
[b] *Corporate Strategic Research Labs., ExxonMobil Research and Engineering Co., Annandale, NJ 08801, USA*

Abstract

This paper aims to gain a better understanding of the flash atomization of a hydrocarbon solution containing *n*-hexadecane and *n*-butane, with nitrogen as the propellant gas. The nitrogen flow rate, injection temperature, and butane concentration were varied. Breakup pattern and spray quality were characterized by taking images at the nozzle exit. Mean droplet diameters were measured as a function of operating conditions. It is shown that the atomization of *n*-hexadecane can be significantly enhanced by using butane as a propellant liquid. For a given mean drop size, the presence of butane can markedly reduce the propellant-gas-to-liquid ratio. A simple and practical correlation for the Sauter mean diameter was developed, taking the form SMD (μm) $= 118.4 - 28.3(\Delta T^* - K)$ where ΔT^* and K are a dimensionless degree of superheating and the cavitation number, respectively. This correlation collapses all the data under diverse conditions into a single curve.
© 2004 Elsevier Ltd. All rights reserved.

Keywords: Binary hydrocarbon atomization; Flash atomization; Cavitation-enhanced atomization; Drop size correlation

1. Introduction

It is well known that flash atomization can be initiated when a pure liquid, a liquid with dissolved gas, or a liquid mixture is subjected to sufficient superheating (boiling) or pressure reduction (cavitation) that causes bubble formation. The subsequent growth of the bubbles drives the atomization process. This process may be used to enhance atomization where the conventional

---

* Corresponding author.
E-mail address: chigier@andrew.cmu.edu (N. Chigier).

pressurized liquid injection cannot achieve the desired fine sprays. This is especially true for injecting heavy hydrocarbons or oils subject to pressure and/or propellant gas constraints. Such is the case, for instance, in the fluid catalytic cracking process which is the primary conversion process in petroleum refining (Veruto and Habib, 1979).

Many prior studies of the flash atomization process dealt with pure liquids. Brown and York (1962) studied the breakup zone of flashing sprays from water and freon-11 jets by high-speed silhouette photography. They concluded that high pressures and high velocities are not necessary for the process, although superheating must be provided. They indicated that the mean drop sizes decrease slightly with increasing jet Weber number at a given temperature and hence at the same bubble growth rate. A slight decrease was also seen with increasing temperature and bubble growth rate when the jet Weber number was approximately constant. Essentially, flash-boiling atomization is initiated through in situ bubble nucleation followed by bubble growth. Oza (1984) investigated the mechanisms responsible for flash boiling and showed spray images of propane, methanol, and indolene fuel injection through an electromagnetic injector. He identified two regimes of flash-boiling injection: (1) flashing with an essentially constant spray-cone angle and (2) flashing with an external expansion. The first was attributed to flash boiling within the injector. The increase in spray-cone angle observed in the second regime is a result of external expansion of the two-phase flow. In an attempt to develop an efficient flash evaporator, Miyatake et al. (1985) examined the effect of injecting bubble nuclei on the flashing of a superheated liquid jet through liquid electrolysis at the nozzle inlet. Kurschat et al. (1992) investigated the evaporation of highly superheated liquid jets. They modelled the evaporation as a sonic deflagration followed by an axisymmetric supersonic expansion for a rough comparison with experimental results. Park and Lee (1994) identified two flashing modes with transparent nozzles of different length-to-diameter ratios (L/D). The first, called the internal mode, is characterized by the formation of two-phase flow inside the nozzle. The other is the so-called external mode where the phase change occurs outside the nozzle. They suggested a critical L/D of seven for the transition between the two modes. They measured drop sizes and spray angle within the bubbly flow regime for flash atomization. They presented the Sauter mean diameter (SMD) as a decreasing function of the extent of superheating.

Flash atomization can also be achieved by dissolving a flashing liquid (or liquid propellant) in the base liquid to be atomized. When the initially subcooled binary liquid is suddenly depressurized sufficiently below the bubble point, the liquid propellant will flash. Sher and Zeigerson-Katz (1996) correlated the SMD of a flashing spray with the initial conditions of a binary mixture of toluene (the base liquid) and freon-22 (the propellant) by using an energy balance approach. For constant process efficiency, the SMD of the thus-generated droplets decreases with increasing propellant mole fraction and with increasing initial injection temperature. Zeigerson-Katz and Sher (1998) then investigated the effect of the injection system on spray characteristics. They found that the SMD decreases with a modified Jakob number. By using this Jakob number they can collapse all data gathered at three different temperatures into a single curve. Kessler et al. (1998) photographed flash atomization of single (preheated dodecane) and binary (preheated 50/50 decane–tetradecane mixture) hydrocarbon fuels. Hitron et al. (1999) atomized an acetone–water solution, with acetone serving as the flashing fluid. With an $L/D = 7$, they were able to distinguish cavitation-enhanced atomization vs. boiling-enhanced atomization. Extending Hitron et al.'s (1999) work, Gemci et al. (2001a,b) performed parametric studies of combined feed of

binary mixtures with the propellant gas (nitrogen) and found that the presence of the flashing fluid can markedly reduce the amount of propellant gas required for the same mean drop size.

If the internal flow conditions are such that stable cavitation bubbles can form, then such bubbles should promote the atomization of the base liquid. The details of the cavitation phenomenon have been studied extensively (Knapp et al., 1970; Brennen, 1995; Shah et al., 1999). Cavitation may occur through the formation of bubbles or cavities in the liquid or it can be a result of the enlargement of the cavities that are already present in the bulk liquid. These bubbles may be suspended in the liquid or may be trapped in tiny cracks at the liquid–solid interface (Shah et al., 1999). He and Ruiz (1995), Mansour et al. (1998), Tamaki et al. (1998), and Tamaki et al. (2001) investigated the cavitation effect on atomization. He and Ruiz (1995) conducted an experimental study on the distribution of the mean velocity and turbulence intensity in both cavitating and noncavitating flows in an injector orifice. Mansour et al. (1998) studied experimentally and numerically the effects of the Hartman cavity on the performance of an ultrasonic gas atomizer used for aluminium spray forming. Tamaki et al. (1998) conducted experimental studies of enhancing atomization through cavitation inside the nozzle.

The acetone–water system used by Hitron et al. (1999) and Gemci et al. (2001a, 2004) may not be a representative model system for many atomization processes of practical interest involving hydrocarbon liquids. In light of this, we used a hydrocarbon model system consisting of two completely miscible liquids in this study: *n*-butane (C_4H_{10}) and hexadecane ($C_{16}H_{34}$). Specifically, we addressed the effects of *n*-butane, propellant gas (nitrogen), and the nozzle internal conditions on hexadecane atomization. Spray images were captured to shed some light on the manner in which cavitation- and boiling-enhanced flash atomization. Significantly, a unifying drop size correlation for flash atomization is developed that reflects the combined effect of cavitation and superheating. It may be used for rational design of flash injectors.

2. Cavitation vs. boiling

Both cavitation- and boiling-enhanced flash atomization are initiated through in situ bubble formation in a liquid mixture. Bubble creation via cavitation can be achieved by changing the nozzle geometry such as the orifice L/D ratio, the inlet corner radius, and the flow velocity in the orifice. Although the basic mechanics of cavitation and boiling are similar, it is important to differentiate the two thermodynamic paths preceding the formation of vapor, as set forth in Brennen (1995).

- A liquid at constant temperature could be subjected to a decreasing pressure, P, which falls below the saturated vapor pressure, P_v. The value of $(P_v - P)$ is called the tension, ΔP, and the magnitude at which rupture occurs is the tensile strength of the liquid, ΔP_c. The process of rupturing a liquid by decrease in pressure at roughly constant liquid temperature is often called *cavitation*.
- A liquid at constant pressure may be subjected to a temperature, T_{inj}, in excess of the normal saturation temperature, T_{sat}. The value of $\Delta T = T_{inj} - T_{sat}$ is the *superheat*, and the point at which vapor is formed, ΔT_{crit}, is called the critical superheat. The process of rupturing a liquid by increasing the temperature at roughly constant pressure is often called *boiling*.

The cavitation number K is often defined as

$$K = \frac{P_o - P_v}{\frac{1}{2}\rho_T U^2} \tag{1}$$

Here P_o and P_v are the downstream pressure (for an emerging jet flow from a nozzle it is the atmospheric ambient pressure) and the vapor pressure of the medium (liquid and propellant gas mixture) in the nozzle orifice, respectively; ρ_T is the overall density of the gas and liquid medium; and U is the average velocity of the medium at the nozzle orifice exit (see Fig. 1). The higher the cavitation number K, the less likely cavitation is to occur; that is, K measures the resistance of the flow to cavitation (Shah et al., 1999). For a given system, cavitation will occur if K becomes less than a critical value K_c; that is, $K < K_c$. He and Ruiz (1995) derived K_c for an orifice. Between the vena contracta and the orifice exit, the steady-state integral momentum equation gives (see Fig. 1 for the notation)

$$P_o - P_c = \rho_T U(U_c - U) - \frac{1}{2}\rho_T U^2 f_{TP}\frac{L}{D} \tag{2}$$

where P_c is the pressure at the vena contracta and f_{TP} is the friction coefficient for the two-phase flow. Right at the moment when cavitation occurs, the pressure in the recirculation region becomes equal to the effective vapor pressure P_v, and the region is filled with a vapor phase. Setting $P_c = P_v$ in Eq. (2), we obtain

$$K_c = 2\left(\frac{1}{C_c} - 1\right) - f_{TP}\frac{L}{D} \tag{3}$$

where $C_c = U/U_c$ (or $C_c = A_c/A$), the contraction coefficient. This contraction coefficient depends primarily on the inlet geometry. For a square-edged orifice a two-dimensional potential flow theory gives $C_c = \pi/(\pi + 2) = 0.611$ (He and Ruiz, 1995). A constant value of $f_{TP} = 0.003$ is used for the two-phase friction coefficient suggested by Allen (1951) for the low pressure flashing steam-water flows through pipes and valves. Setting $C_c = 0.611$, $f_{TP} = 0.003$, and $L/D = 7$, we obtain $K_c = 1.25$ for the nozzle orifice used in the present experiment.

In the absence of cavitation, one can achieve flash atomization by relying on superheating the working fluid followed by expansion through a nozzle. To improve atomization of high-boiling liquids, one can dissolve a small amount of a low-boiling liquid propellant in the base liquid. The resulting binary solution is then heated before being injected through a converging nozzle. By
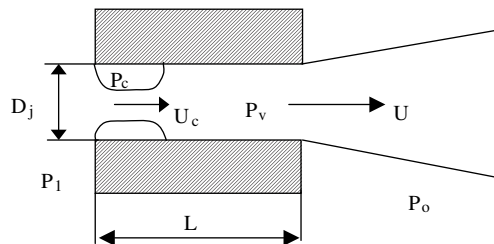

Fig. 1. Schematic of the flow in a cavitating nozzle orifice.

forcing the rapid vaporization of the lighter component in the solution, the number of bubbles will increase rapidly. Flashing is initiated when this binary liquid mixture is exposed to a sudden pressure drop below the saturation vapor pressure at the prevailing temperature, causing nucleation and formation of vapor bubbles. The subsequent growth of the vapor bubbles drives the atomization of the base liquid.

A flashing process is often identified with a critical superheat-temperature difference, above which complete flashing occurs with no remaining segments in the liquid phase. The superheat-temperature difference (*superheat degree*, ΔT) can be defined as the difference between the measured temperature of the liquid leaving the nozzle (T_{inj}) and its bubble-point temperature (T_{sat}) corresponding to the ambient pressure (P_o). That is, $\Delta T = T_{inj} - T_{sat}(P_o)$. Alternatively, a dimensionless superheat degree, ΔT^*, is also often used as a measure of the extent of superheating:

$$\Delta T^* = \frac{\Delta T}{\Delta T_{crit}} = \frac{T_{inj} - T_{sat}(P_o)}{T_{sat}(P_{inj}) - T_{sat}(P_o)} \tag{4}$$

Some of the important properties of a liquid propellant as a promoter for flash atomization are a high specific heat, a low heat of vaporization, and a low boiling point (Zeigerson-Katz and Sher, 1998).

3. Experimental setup

As Fig. 2 shows, the experimental equipment consists of a pressurized binary liquid cylinder, a pipeline heater, a pressurized cylinder of nitrogen, and the atomizer. The two different binary mixtures (2 and 5 wt.% *n*-butane in hexadecane) were made by blending under special conditions because *n*-butane is a vapor at ambient conditions. The liquid is heated in a pipeline heater with a precise voltage control unit. The heating is gradually increased until the desired injection temperature is reached and a stabilized heating of the liquid solution is accomplished. Upstream of
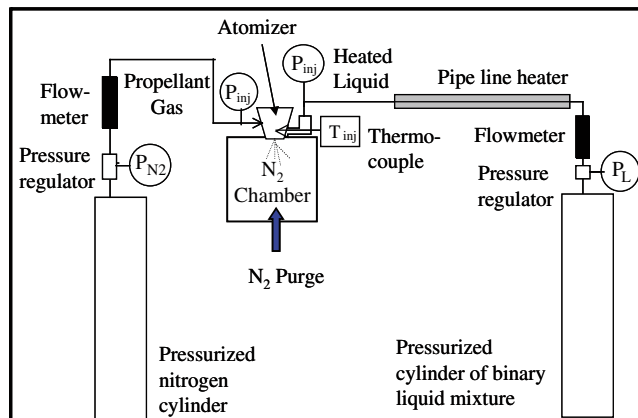

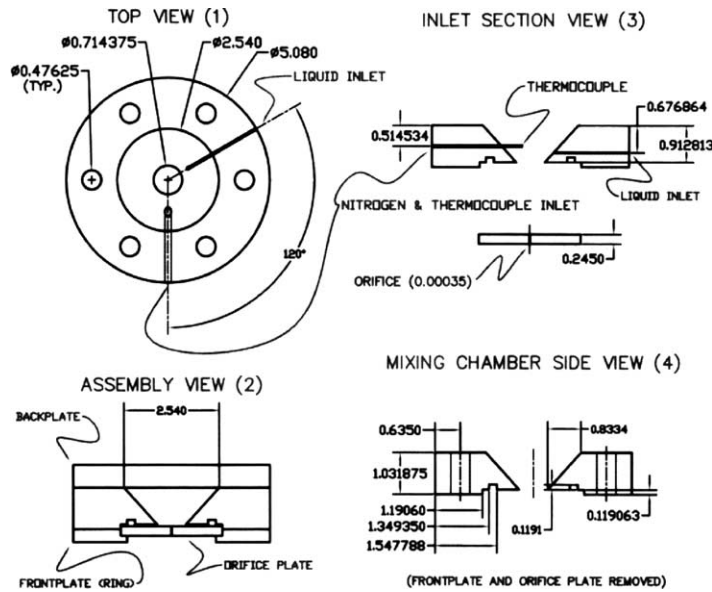Fig. 2. Experimental setup for the cavitation enhanced flash atomization.

Fig. 3. Details of the nozzle and orifice geometry.

the nozzle orifice, the heated binary liquid solution and the propellant gas were fed into a mixing chamber, as shown in Fig. 3. The conical mixing chamber has a depth of 9.5 mm with a top cone diameter of 25.4 mm. This decreases to 7.1 mm at the bottom of the cone in the mixing chamber. The orifice plate has an exit diameter 350 μm and a thickness of 2.45 mm (seven times the orifice diameter). This plate is fixed to the bottom of the mixing chamber. The detail dimensions of the nozzle are given in Fig. 3.

To create stable cavitation bubbles, we used a sharp angle orifice plate with a relatively long L/D of 7. This was based on Hitron et al.'s study (1999) which indicated that among the three L/D's (1.4, 2.4, and 7) used, $L/D = 7$ gave the most pronounced cavitation effect. Referring to Fig. 2, the injection pressure P_{inj} was measured with pressure gauges located at the nozzle inlet both in the liquid and nitrogen lines and the two pressure readings were very close to each other. The injection temperatures of N_2 and liquid mixture T_{inj} were measured by a thermocouple located inside the mixing chamber of the atomizer. The thermocouple was inserted into the chamber through the liquid inlet pipe. The heating of nitrogen is accomplished in the mixing chamber. Nitrogen was used as the propellant gas instead of air for safety reasons. The flow inside the nozzle orifice for all test conditions is completely bubble flow based on the two-phase flow correlation given in Perry's Chemical Engineers' Handbook (Perry and Green, 1984).

The flashing spray was injected into a plexiglas N_2 chamber, which has openings on both sides for the CCD camera and strobe light. We purged nitrogen into the N_2 chamber and prevented ambient air from entering into the N_2 chamber. The *n*-butane vapor was mixed with 11.2 l/min of purging nitrogen, so its concentration was well below the lower explosion limit of 2%. The unvaporized liquid spray was collected through a funnel into a disposal flask at a distance far below
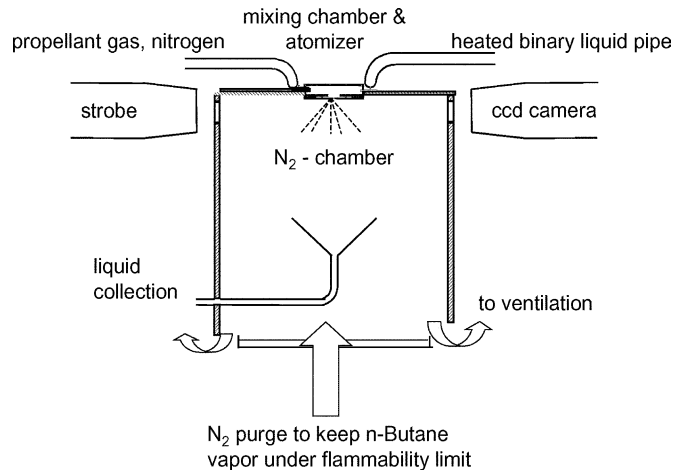
Fig. 4. Experimental setup for the imaging system (Greenfield Speedview #700).

the nozzle exit. The vapor and nitrogen were forced to leave the plexiglas N_2 chamber through the ventilation openings and were sucked out of the hood by the exhaust ventilation system. Images of the spray breakup and the spray pattern were taken at the nozzle exit with the Greenfield Speedview #700 imaging system, which was located inside a ventilation hood (Fig. 4). This instrument was also used for drop size measurements taken at 3 cm downstream of the nozzle exit. In the Greenfield image analyzer the 8 µm/pixel resolution with an image size of 5.1 mm × 3.8 mm is used for the drop size measurement. The minimum detectable drop size at this resolution level is 22 µm.

The Greenfield Image Analyzer consists of a TV camera containing a CCD sensor, a strobe light, interchangeable microscope lenses, digital imaging hardware and software. The digital camera contains an array of light-sensitive elements which are synchronized with the intense flash of the strobe light. The strobe is synchronized with the video signal. A xenon flash lamp is used for the strobe light to freeze images on the sensor. It has a flash duration of less than 0.5 µs which is sufficiently short to freeze particle images over the injection velocity range of the experiments (75 m/s). The CCD camera and strobe light face each other while the system being analyzed is placed in between. The light from the strobe comes from behind the system, causing the camera to pick up backlight, and thus illuminating the system. As a result, the droplets appear as black dots on a white background. The analyzable size range is between 5 and 6000 µm, with a maximum speed of 30 frames/s. The Fraunhofer diffraction based particle size analyzer was not used for the size measurement because the hot gases and liquids and vaporized gas phases would cause beam steering.

Table 1 lists the test conditions where Q_{N_2} and Q_L are the volumetric flow rates of nitrogen and liquid (single or binary) mixture and W_{but} is the weight % of butane in hexadecane. As seen, two N_2-to-liquid volumetric flow rate ratios, defined as $r = Q_{N_2}/Q_L$, of 5 and 10 were used to study the effect of the propellant gas on the atomization of pure hexadecane and two different butane–hexadecane solutions. The measurements for each r were conducted at three different injection temperatures: 80, 100, and 120 °C.

Table 1
Test conditions of the binary hexadecane–butane solutions

$r = \frac{Q_{N_2}}{Q_L}$	Q_L (cm^3/min)	T_{inj} (°C)	P_{inj} (kPa)		
			$W_{but} = 0\%$	$W_{but} = 2\%$	$W_{but} = 5\%$
5	40	80	156	184	232
5	40	100	170	212	239
5	40	120	239	246	253
10	40	80	198	225	239
10	40	100	212	246	253
10	40	120	246	253	260

4. Results

4.1. Thermophysical properties

Table 2 shows the estimated thermodynamic and physical properties of pure hexadecane and the two butane–hexadecane solutions in the absence of N$_2$. The liquid density (ρ_L), viscosity (μ_L), and surface tension (σ_L) decrease with increasing temperature. Fig. 5 shows the results of vapor–liquid equilibrium calculations at ambient pressure and three different injection pressures. Adding a small amount of *n*-butane (2 wt.%) can significantly reduce the bubble point. The reduction becomes progressively smaller upon further addition of *n*-butane.

The combined feed of the propellant gas (N$_2$) and the liquid (single or binary solution) has totally different thermodynamic characteristics than the liquid-only feed. The volumetric flow rates of the gas and liquid solutions were measured at standard conditions before the pipeline heater. The liquid flow rate was kept constant at $Q_L = 40 \times 10^{-6}$ m^3/min (Std) (Std refers to standard conditions at $T_o = 15.6$ °C and $P_o = 101.33$ kPa) while the N$_2$ propellant gas was mixed in the nozzle chamber with a flow rate that gives $r = 5$ or 10. Flash calculations were performed for the combined feeds based on the liquid flow rate $Q_L = 1$ m^3/h (Std). As an example, Table 3 shows the calculation results for the 95/5 hexadecane–butane ($W_{but} = 5\%$) solution at $r = 10$ and $T_{inj} = 120$ °C. Note that the results also include the overall density, surface tension, and viscosity for the combined feed (gas–vapor–liquid or gas–liquid mixture). From these physical properties,

Table 2
Flash boiling characteristics of the binary hexadecane–butane solutions for $r = 0$ (no N$_2$ present)

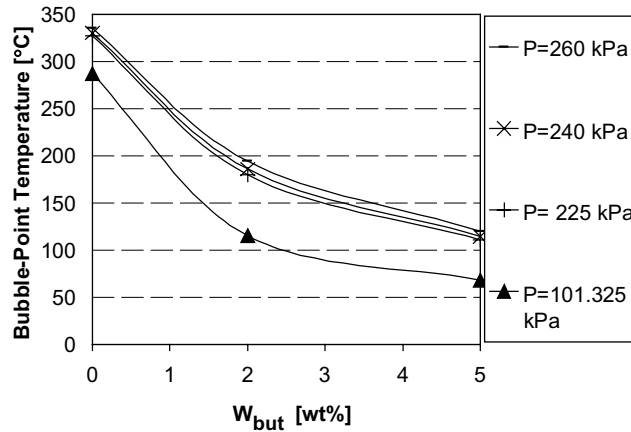| W_{but} (%)	T_{inj} (°C)	P_v (kPa)	ρ_L (kg/m^3)	μ_L (mPa s)	σ_L (mN/m)
0	80	0.020	731.7	1.177	22.29
0	100	0.091	717.7	0.9088	20.61
0	120	0.304	703.6	0.7241	18.99
2	80	55.12	728.2	1.075	21.91
2	100	79.54	714.1	0.836	20.19
2	120	109.13	699.8	0.671	18.53
5	80	130.20	722.6	0.944	21.32
5	100	188.26	708.1	0.743	19.54
5	120	258.98	693.6	0.601	17.82

Fig. 5. Bubble-point temperature vs. wt.% *n*-butane in hexadecane at different injection and ambient pressure (no N_2 present).

Table 3
An example of thermodynamic equilibrium calculation for $W_{but} = 5\%$ and $r = 10$ (10 Std m³/h for N_2 and 1 m³/h for liquid) at $T_{inj} = 120$ °C

Stream 1:	Pure N_2	at 15.6 °C	1.00 atm-a	10.00 Std m³/h
Stream 2:	$95C_{16}\_5C_4$	at 15.6 °C	1.00 atm-a	1.00 m³/h (Std)
Flash specs	Temp/pres			
Fraction liquid (M)	0.8109			
Fraction liquid (Wt)	0.9552			
Fraction liquid (LV)	0.94			
			Temperature (°C)	120
			Pressure, abs. (kPa)	260
			Duty (kW)	54.4376
			Fraction vapor (M)	0.1891
			Fraction vapor (Wt)	0.0448
			Fraction vapor (LV)	0.06

Stream properties at flash conditions—for combined feeds

| Property	Total	Liquid	Vapor
Mole flow (kmol/h)	4.284	3.474	0.81
Mass flow (kg/h)	775.8	741	34.77
Molecular weight	181.0749	213.2857	42.919
Density (kg/m³)	69.45	699.7	3.438
Molar volume (m³/kmol)	2.607	0.3048	12.48
Mole enthalpy (kJ/kmol)	−319 276.5	−380 889.4	−55 011.6
Mass enthalpy (kJ/kg)	−1763.2	−1785.8	−1281.8
Flowing enthalpy (kW)	−380	−367.6	−12.38
Entropy (kJ/kmol K)	−1206.9	−1450.3	−163.1
Viscosity (mPa s)		0.6682	0.0136
Specific gravity (@STP)	0.7597	0.7719	
Surface tension (mN/m)	18.38		
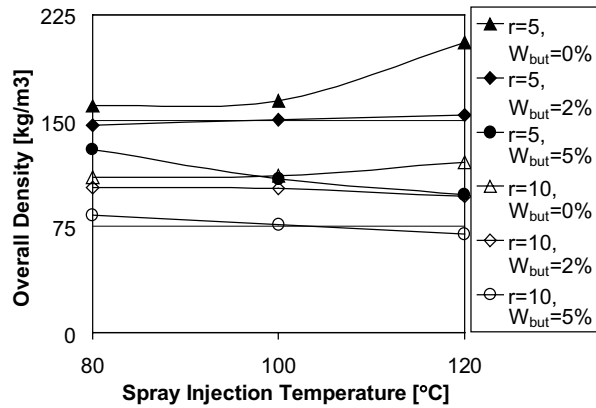
Fig. 6. Overall density of combined feed of N_2 and liquid solution as a function of T_{inj}.

one can calculate the total mass flow rate ($\dot{m}_T$) and the jet exit velocity. Take the binary liquid feed at $r = 10$ as an example, $\dot{m}_T = 775.8$ kg/h for $Q_L = 1$ m³/h (Std) and $\dot{m}_T = 1.86$ kg/h for $Q_L = 2.4 \times 10^{-3}$ m³/h (Std).

Fig. 6 shows the overall density of the combined feed as a function of the injection temperature at different r values. As can be seen, the overall density can be an increasing or decreasing function of the injection temperature, depending on r and W_{but}. The overall viscosity and overall surface tension decrease slightly in the presence of N_2. Fig. 7 shows the calculated jet velocity emerging from the nozzle orifice as a function of T_{inj} for different r and W_{but}. The jet exit velocity U of the two-phase flow is calculated based on the mass flow rate of the combined feed (with N_2) and the binary liquid solution as follows:

$$U = \frac{\dot{m}_T/\rho_T}{\pi D_j^2/4} \tag{5}$$
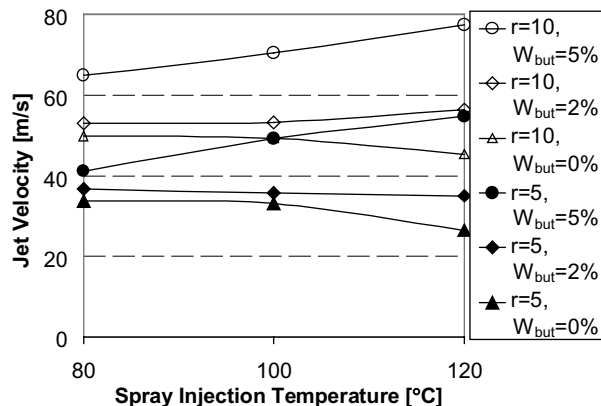
Fig. 7. Jet velocity vs. injection temperature T_{inj}.

The jet velocity increases with increasing injection temperature for $W_{but} = 5\%$ at both $r = 5$ and 10, apparently due to the contribution of the increased butane vapor. The jet velocity stays relatively constant for $W_{but} = 2\%$. In contrast, the jet velocity for the hexadecane-N_2 feed decreases as the injection temperature approaches 120 °C due to an increase in the overall density of the hexadecane-N_2 mixture. Note that the hexadecane density decreases from 731.7 to 703.6 kg/m^3 in going from 80 to 120 °C.

4.2. Dimensionless groups

The jet velocity is used for calculating K, jet Reynolds number (Re_j) and jet Weber number (We_j). The jet Reynolds number for the gas–liquid mixture is calculated based on the jet velocity, the nozzle exit diameter (D), and the overall density (ρ_T) and viscosity (μ_T) of the feed:

$$Re_j = \frac{UD\rho_T}{\mu_T} \tag{6}$$

Fig. 8 shows that there is an apparent linear relationship between Re_j and the injection temperatures at different r and W_{but} values. At $T_{inj} = 80$ °C, Re_j varies between 1615 and 1867, while it varies between 2628 and 2846 at $T_{inj} = 120$ °C. The images corresponding to these Reynolds numbers show that the jet flow appears to have both semi-turbulent and turbulent characters. For pure liquid jets, the critical Reynolds number (Re_{crit}) at which the jet changes from laminar to turbulent flow is given by the following empirical correlation (Lefebvre, 1989).

$$Re_{crit} = 12\,000\left(\frac{L}{D}\right)^{-0.3} \tag{7}$$

Extrapolating this correlation to gas–liquid two-phase flow gives $Re_{crit} = 6693$ for the nozzle used in the present study.

The spray jet issuing from the nozzle orifice tip undergoes primary and secondary atomization. The term primary atomization is used for the disintegration process of the liquid jet. The sec-
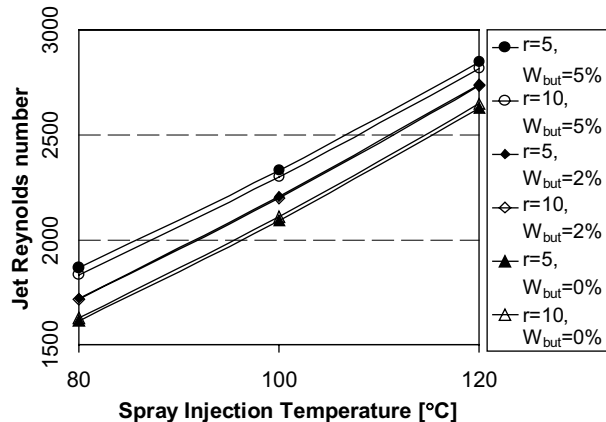

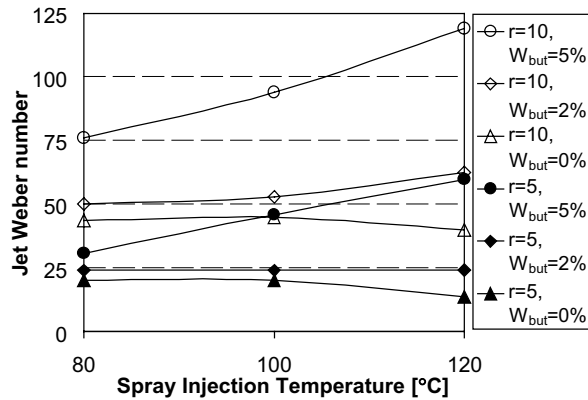Fig. 8. Jet Reynolds number vs. injection temperature T_{inj}.

Fig. 9. Jet Weber number vs. injection temperature T_{inj}.

ondary atomization involves further breakup of droplets when the aerodynamic forces acting on the drop surface overcome the droplet surface forces. The critical condition for disintegrating the liquid jet is characterized by We_j, which is defined as the ratio the impact stress of the gas phase on the interface to the normal stress caused by the interfacial tension acting on any cross section.

Figure 9 shows the jet Weber number (We_j) as a function of T_{inj} at different r and W_{but} values. The jet Weber number is calculated based on the combined feed of N_2 and binary liquid solutions as follows:

$$We_j = \frac{\rho_g U^2 D}{\sigma_T} \tag{8}$$

where ρ_g is the ambient gas density calculated at the average temperature between T_{inj} and T_o and σ_T is the overall surface tension of the binary liquid solution when N_2 is present. Increasing the N_2-to-liquid ratio increases the jet Weber number for all cases. The lowest jet Weber number is 13.7, corresponding to pure hexadecane ($W_{but} = 0\%$) at $T_{inj} = 120$ °C and $r = 5$. This value is comparable to the critical Weber number for the single-phase value of $We_{crit} = 13$. Above the critical Weber number droplet breakup occurs. It bears emphasizing that the critical Weber number is given for the single-phase liquid jet whereas in our experiment we deal with a two-phase jet flow of gas and binary liquid solution.

4.3. Jet breakup and spray images

The task here is to examine the extent to which the flashing butane can promote the base liquid atomization with a reduced amount of the propellant gas. The injection temperature T_{inj} for the single liquid atomization was far below the saturation temperature at the ambient pressure (temperature differences as superheat degree are $\Delta T = -206.9$ °C for $T_{inj} = 80$ °C and $\Delta T = -166.9$ °C for $T_{inj} = 120$ °C). For the binary liquid atomization with $W_{but} = 2\%$, the extent of superheating is relatively insignificant even at 120 °C, about 4.9 °C above the bubble-point temperature. All injection temperatures for $W_{but} = 5\%$ were above the bubble point, with $\Delta T = 12.1$ and 52.1 °C, respectively for $T_{inj} = 80$ and 120 °C. An important point to note here is

that the injection temperatures for all binary mixtures were far below the boiling point of hexadecane.

Figs. 10 and 11 show the imaging results obtained in the Greenfield experiments taken at the nozzle exit. The drop size measurements were made at 3 cm downstream of the nozzle exit. At this location the primary breakup process was seen to be essentially completed and there were no discernable liquid ligaments. Each figure is a two-dimensional array. Looking across the same row
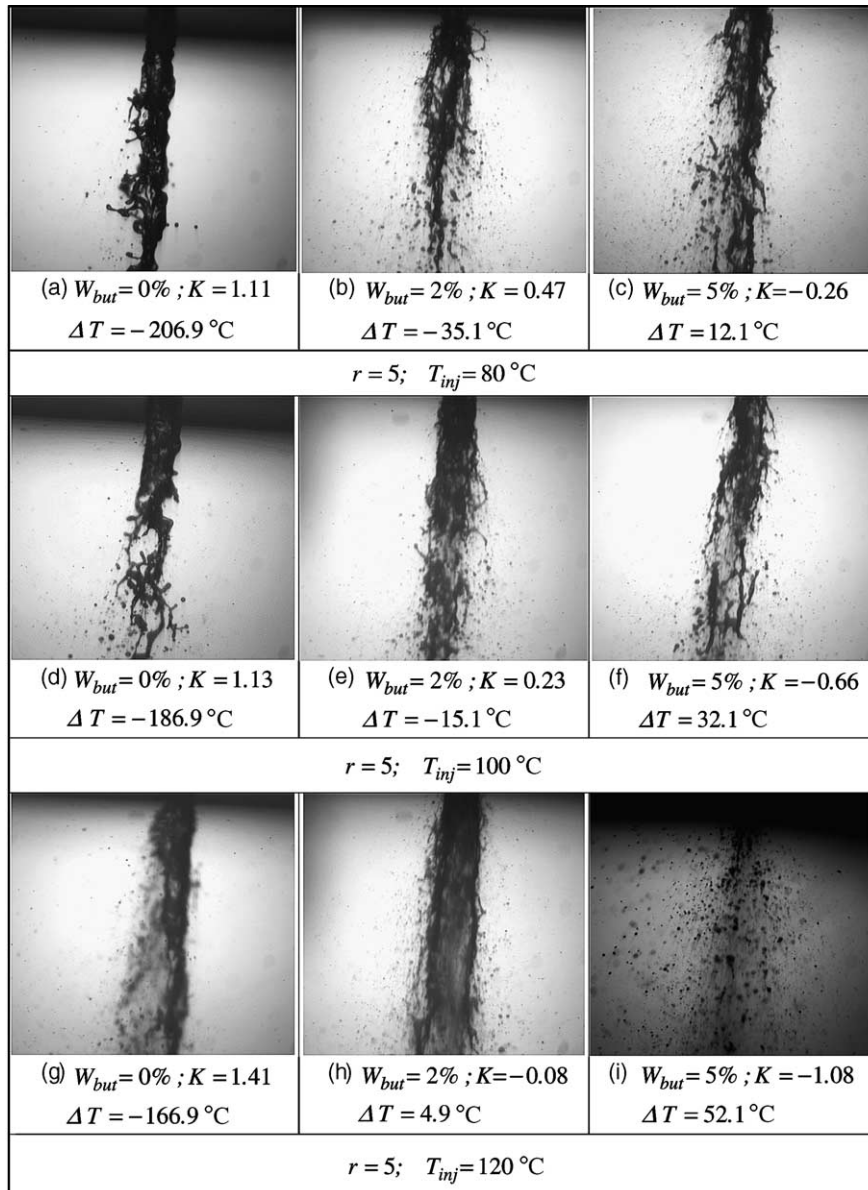

Fig. 10. Spray images for N_2-to-liquid ratio of $r = 5$.

allows one to see the effect of liquid propellant concentration. Looking down across the column gives the effect of increasing temperature. Comparing the images of the same row and column numbers in Figs. 10 and 11 constitutes the third dimension, which shows the effect of gas propellant (e.g., cf. Figs. 10e and 11e for $r = 5$ and 10 at otherwise identical conditions, respectively).

| (a) $W_{but} = 0\%$; $K = 0.74$ | (b) $W_{but} = 2\%$; $K = 0.32$ | (c) $W_{but} = 5\%$; $K = -0.17$ |
| $\Delta T = -206.9\,^{\circ}\mathrm{C}$ | $\Delta T = -35.1\,^{\circ}\mathrm{C}$ | $\Delta T = 12.1\,^{\circ}\mathrm{C}$ |

$r = 10$; $T_{inj} = 80\,^{\circ}\mathrm{C}$

| (d) $W_{but} = 0\%$; $K = 0.75$ | (e) $W_{but} = 2\%$; $K = 0.15$ | (f) $W_{but} = 5\%$; $K = -0.46$ |
| $\Delta T = -186.9\,^{\circ}\mathrm{C}$ | $\Delta T = -15.1\,^{\circ}\mathrm{C}$ | $\Delta T = 32.1\,^{\circ}\mathrm{C}$ |

$r = 10$; $T_{inj} = 100\,^{\circ}\mathrm{C}$

| (g) $W_{but} = 0\%$; $K = 0.82$ | (h) $W_{but} = 2\%$; $K = -0.05$ | (i) $W_{but} = 5\%$; $K = -0.76$ |
| $\Delta T = -166.9\,^{\circ}\mathrm{C}$ | $\Delta T = 4.9\,^{\circ}\mathrm{C}$ | $\Delta T = 52.1\,^{\circ}\mathrm{C}$ |

$r = 10$; $T_{inj} = 120\,^{\circ}\mathrm{C}$

Fig. 11. Spray images for N_2-to-liquid ratio of $r = 10$.

Also shown in Figs. 10 and 11 are values of ΔT and K for each condition. In what follows we discuss the qualitative features of each effect individually.

Typically, we took 3–4 images at each set of test conditions. We adjusted the contrast and brightness of the image to estimate ligament lengths on a relative basis. The ligament lengths were later quantified from the average drop size measurements, which are the result of an ensemble average of hundreds of frames.

4.3.1. Effect of liquid propellant

The images shown in Figs. 10 and 11 indicate that for a given set of r and T_{inj}, the n-butane addition shortens the breakup length and promotes secondary atomization. The effect is more pronounced for the changeover from pure hexadecane to the $W_{\text{but}} = 2\%$ solution at the low T_{inj} of 80 °C. In this case the system is subcooled (with $\Delta T = -206.9$ and -35 °C). Thus, cavitation appears to be the more important factor responsible for the improved atomization as it increases the injection pressure and velocity.

4.3.2. Effect of injection temperature

While increasing T_{inj} from 80 to 120 °C improves hexadecane atomization for both the single and binary liquids, the improvement is more pronounced for the binary liquid. In the single liquid case, some small disturbances were noted, but the jet was smooth and stable at $r = 5$ and 80 °C (see Fig. 10a). From the images, one can see that the primary breakup length and ligaments get shorter upon increasing the injection temperature or the butane concentration. This observation is consistent with the drop size measurements to be discussed later. At the highest injection temperature of 120 °C, the binary liquid forms a spray essentially at the nozzle exit for $r = 5$ or 10. Presumably, this is caused by intense bubble formation. Note that heating of the binary solution to the injection temperature leads to a higher pressure drop than that of pure hexadecane.

4.3.3. Effect of gas propellant

As shown in Figs. 10 and 11, an increase in r from 5 to 10 enhances the atomization of neat hexadecane with no visible jets at $r = 10$, with the most pronounced effect at 80 °C. For pure hexadecane at a fixed T_{inj}, while increasing r from 5 to 10 does not change ΔT, it raises ΔT^* at 80 °C but barely at 120 °C. By contrast, for the binary solution at a fixed T_{inj}, ΔT and ΔT^* both show little if any effect of r. However, K decreases appreciably as r increases for both single and binary liquids due to an increase in the fluid velocity. Thus, the r-enhanced atomization for the binary liquid can be attributed to cavitation. For pure hexadecane, the enhancement should be attributable in large part to cavitation and in small part to superheating.

4.3.4. Gas and liquid propellant trade-off

The trade-off between the gas and liquid propellants can be seen by comparing the corresponding images in Figs. 10 and 11. For instance, at $T_{\text{inj}} = 120$ °C the binary liquid with $W_{\text{but}} = 5\%$ at $r = 5$ (Fig. 10i) gives rise to a finer spray than the pure liquid at $r = 10$ (Fig. 11g). The two cases have similar injection pressures of 253 and 246 kPa, respectively, see Table 1. Over the conditions tested, the finest spray is obtained at the highest T_{inj}, W_{but}, and r (see Fig. 11i). The key message here is that a propellant can be used to reduce the amount of propellant gas for the

same level of spray quality. The discussions thus far have been qualitative. We next summarize quantitative results.

4.4. Analysis of spray characteristics

Our goal is to develop a general correlation for the SMD in terms of the dominant system dimensionless groups. As a first step, it is instructive to look at the individual effect of K, ΔT^*, We_j, and W_{but} on the SMD. We use ΔT^* as the main parameter characterizing the extent of super-heating because it contains the bubble-point temperature at the injection pressure. An obvious shortcoming of ΔT is that it does not account for the effect of r.

Before presenting the data, a word about the data uncertainty is in order. Using the method of Kline and McClinctock (1953), we estimated the maximum uncertainties for the following dimensionless parameters with a 95% confidence interval: $Re_j = 4.1\%$, $We_j = 6.92\%$, $K = 6.8\%$, $\Delta T^* = 3.6\%$, $r = 3.6\%$, and $L/D = 0.2\%$. Table 4 summarizes the uncertainties of some measured physical properties.

4.4.1. Sauter mean diameter (SMD)

Figs. 12 and 13 plot the SMD as a function of the cavitation number K for $r = 5$ and 10, respectively. Each figure shows the effect of the injection temperature parametrically, so the variation in K for each curve is due to the variation of liquid's n-butane content. Both figures show the expected trend in that the SMD drops with decreasing cavitation number at constant injection temperature. The addition of a small amount of butane (2 wt.%) to hexadecane can markedly reduce the SMD; this effect is particularly pronounced at low temperatures (80 °C) where the boiling-enhanced mechanism (or superheating) plays little, if any, role. The addition of butane increases vapor pressure and also slightly increases the jet velocity in some cases. Not surprisingly, Figs. 12 and 13 show that the beneficial marginal effect of butane addition becomes increasingly weaker with increasing butane content. As mentioned earlier, the critical cavitation number for the nozzle orifice is estimated to be $K_c = 1.25$. Although this K_c value is based on a single-phase theory (but including the two-phase friction coefficient) and may not be applicable to the present

Table 4
Uncertainties for the relevant variables (95% confidence interval)

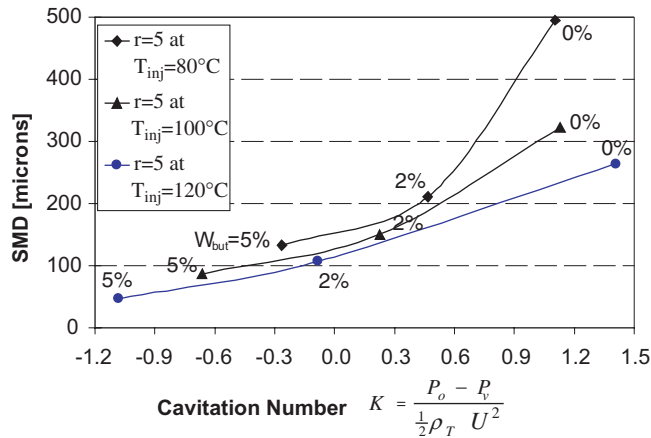| Variables	Uncertainty (%)
Total mass flow rate, $\dot{m}_T$	2.1
Jet exit velocity at nozzle, U	3.1
Sauter mean diameter, SMD	6.0
Surface tension, σ	2.1
Injection pressure, P_{inj}	2.0
Tension $(P_v - P)$, ΔP	2.25
Injection temperature, T_{inj}	0.25
Dynamic viscosity, μ	2.25
Diameter of the jet, D_j	0.1
Overall density, ρ_T	2.25

Fig. 12. SMD vs. cavitation number for $r = 5$.

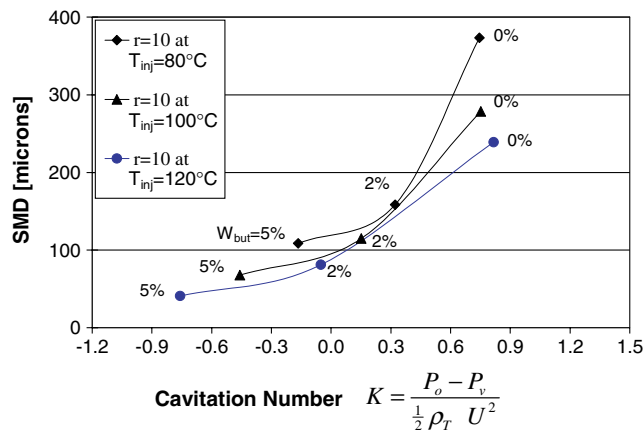Fig. 13. SMD vs. cavitation number for $r = 10$.

case, we take this value as suggesting that it is likely that cavitation occurs ($K < K_c$) under all conditions tested except for the pure liquid case ($W_{but} = 0\%$) at $r = 5$ and $T_{inj} = 120$ °C.

Figs. 14 and 15 show the SMD vs. ΔT^* for $r = 5$ and 10, respectively. The data also exhibit the expected trend. To reduce the SMD, one can add the flashing liquid, increase the superheat degree, and/or increase the propellant gas amount. Remarkably, the SMD for the $W_{but} = 5\%$ binary liquid at the lowest operating severity ($T_{inj} = 80$ °C and $r = 5$) is far smaller than that for pure hexadecane atomized at the highest operating condition ($T_{inj} = 120$ °C and $r = 10$); that is, 133 vs. 238 μm. Also the coarsest drop size, SMD = 494 μm, from hexadecane atomization at $T_{inj} = 80$ °C and $r = 5$ could be reduced to 41 μm by adding 5 wt.% *n*-butane.

Fig. 16 shows that the SMD is a decreasing function of We_j. Increasing the Weber number results in a finer atomization in the primary breakup zone and hence smaller droplets. The plots
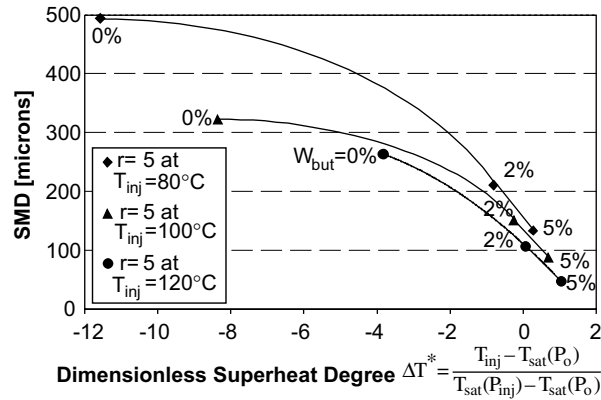
Fig. 14. SMD vs. dimensionless superheat degree ΔT^* for $r = 5$.
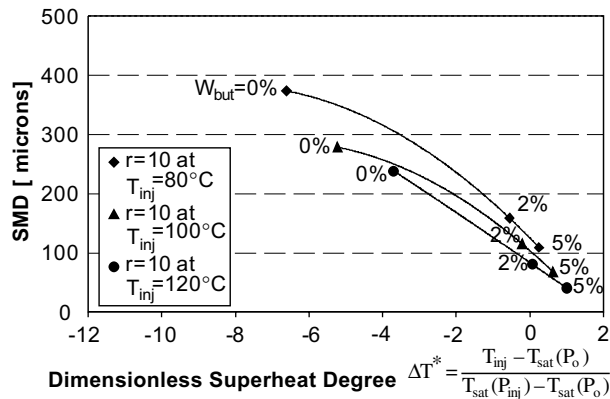
Fig. 15. SMD vs. dimensionless superheat degree ΔT^* for $r = 10$.

really magnify the effect of the butane addition (the changeover from pure hexadecane to the $W_{but} = 2$ wt.% case).

The effect of the butane content is shown in Fig. 17, which reveals the trade-off among the injection temperature, butane content, and r. The flashing liquid can be used to reduce the amount of propellant gas or to decrease the injection temperature for the same SMD. Specifically, one can see this by going horizontally from points A to B. For example, to obtain an SMD of 239 μm, one can inject pure hexadecane at $r = 10$ and $T_{inj} = 120$ °C. The same drop size can also be achieved by adding *n*-butane to hexadecane while reducing the heating or the propellant gas. As shown in Fig. 17, at point B the required drop size is obtained with a butane content of about 1.7 wt.% at the far less severe conditions of $T_{inj} = 80$ °C and $r = 5$.

4.4.2. Cumulative size distributions

Fig. 18 shows the effects of the injection temperature, *n*-butane content, and r on the cumulative volume size distributions for some representative cases. Increasing the injection temperature by
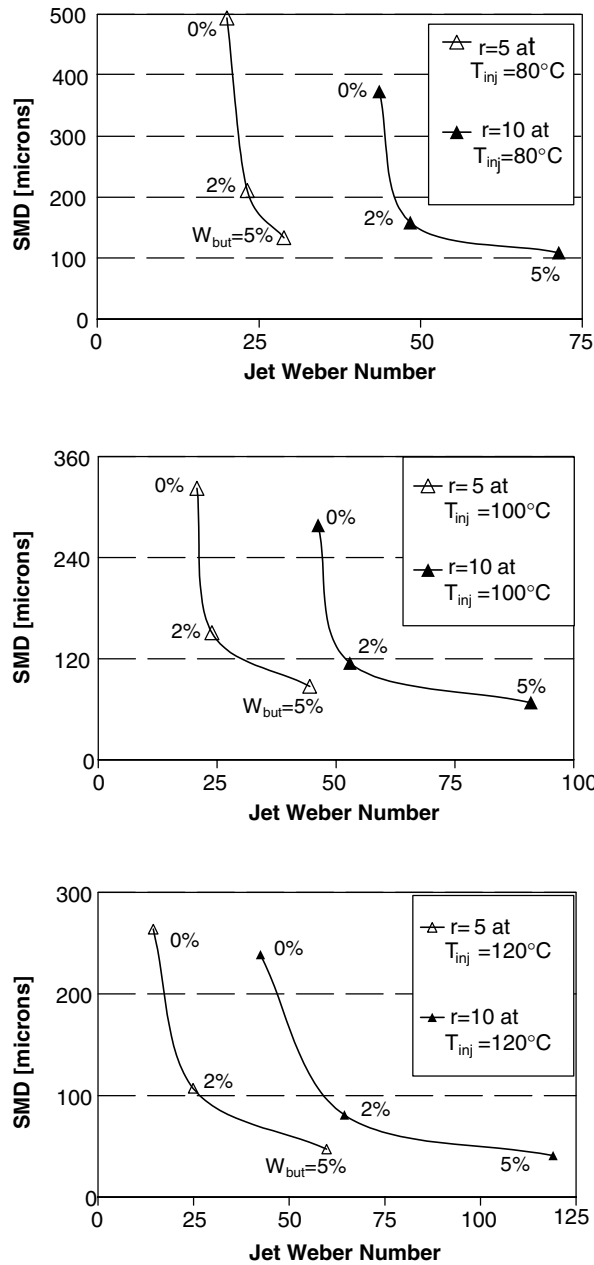
Fig. 16. SMD vs. jet Weber number for different injection temperatures.

40 °C for $W_{but} = 2\%$ and $r = 10$ reduces the maximum drop size from 657 μm with a median size of 254 μm to 429 μm with a median size of 43 μm (see Fig. 18a and b). At $T_{inj} = 80$ °C the spray consists of mainly coarse drops, whereas at $T_{inj} = 120$ °C the drop size distribution shows a maximum at 70 μm. Fig. 18c and d depicts the effect of the liquid propellant on the size
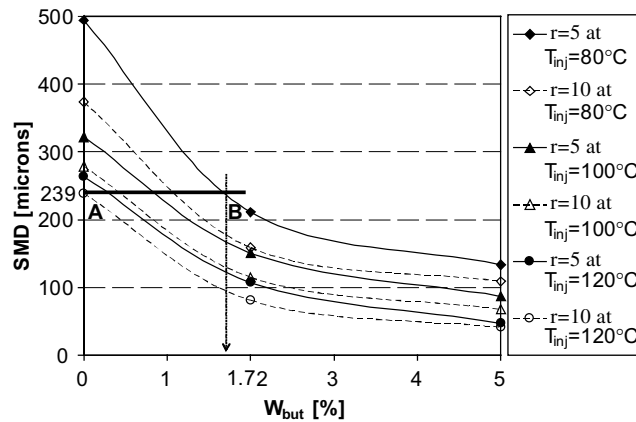
Fig. 17. SMD vs. n-butane content in hexadecane for different r and T_{inj}.

distribution for $r = 10$ and $T_{inj} = 100$ °C. With pure hexadecane (Fig. 18c), the drop size varies between 146 and 1601 μm with a median size of 275 μm. By adding 5% n-butane to hexadecane, the drop size range shifts significantly to a relatively more even and small size range between 22 and 368 μm with a median value of 88 μm (see Fig. 18d). The effect of gas propellant amount on the size distribution can be seen from Fig. 18e and f. Increasing r from 5 to 10 for $W_{but} = 5\%$ and $T_{inj} = 120$ °C reduces the median drop size from 50 to 43 μm.

4.5. Overall correlation

It is highly desirable to be able to develop a correlation that would collapse all the data under diverse conditions. As illustrated elsewhere (Ho, 2003; Ho et al., 1992), this can be done via the following approach. A chemometric analysis (Sharaf et al., 1986) is performed to sift through the following system parameters: W_{but}, r, T_{inj}, P_{inj}, K, ΔT, ΔT^*, Re_j, and We_j. Invariably, some of these parameters correlate with each other (i.e., they are not orthogonal to each other). To eliminate the redundancy, these parameters are *linearly* combined to form a much fewer number of *independent* latent parameters by means of the partial least squares method. For the problem at hand, as it turns out, the dominant features of the flash injection can be approximately projected onto a one-dimensional subspace spanned by a single variable $(\Delta T^* - K)$. This says that despite the hydrodynamic and thermodynamic complexities of the system, the underlying physics is governed by cavitation and superheating. We may add that while this might be expected intuitively, the simplicity of the resulting correlation is a pleasant surprise, as shown next.

On the basis of the forgoing, we construct the following correlation by forming a composite variable FI, called flushing index, that is defined as

$$FI = \Delta T^* - K \tag{9}$$

And we fit the SMD (in μm) data to a linear function of FI. The best fit—with only two fitting parameters for 18 data points—gives
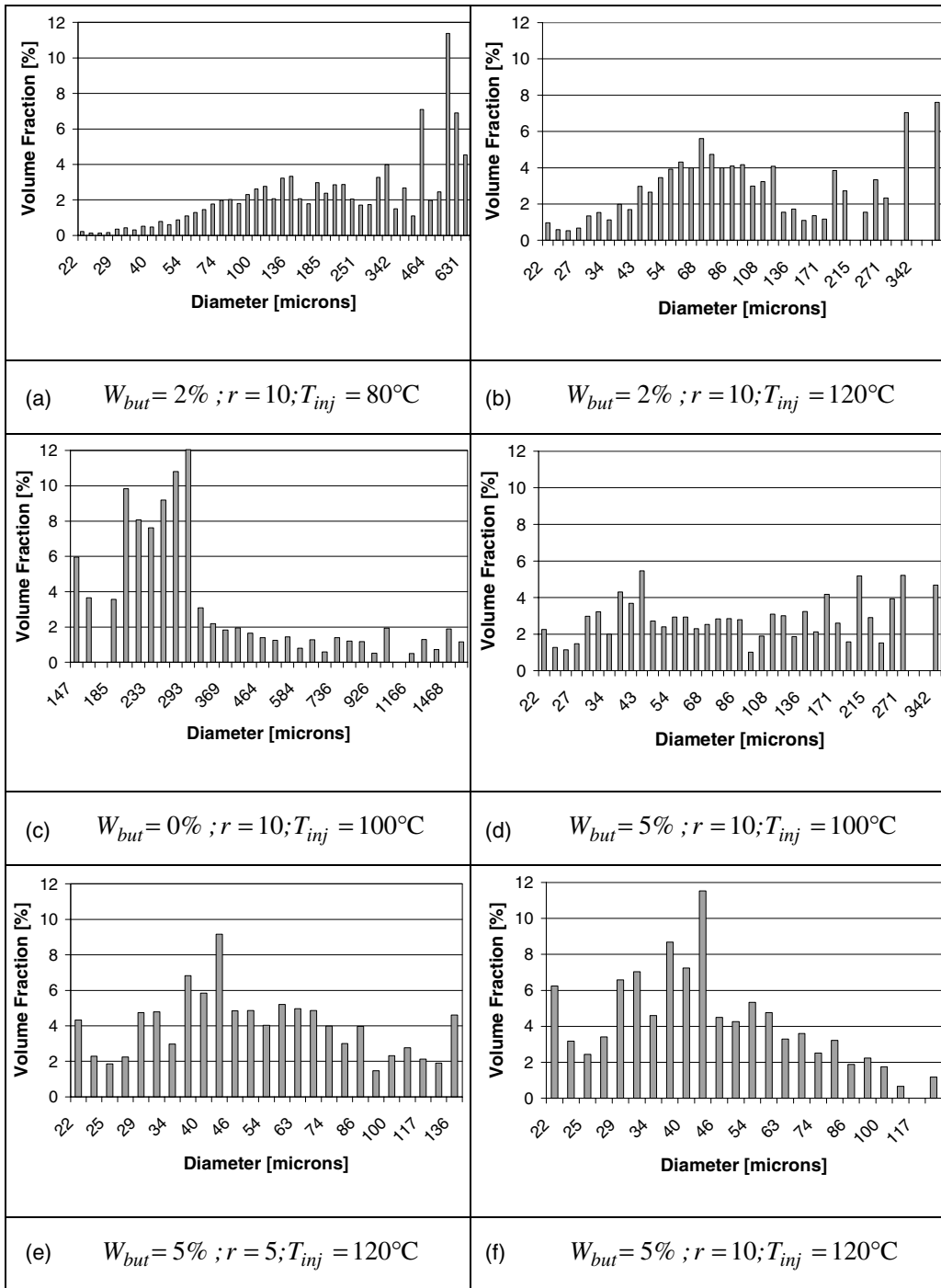
$$SMD = 118.40 - 28.29 FI \tag{10}$$

Fig. 18. Cumulative size distributions: (T_{inj}) effect (frames a and b), W_{but} effect (frames c and d), and r effect (frames e and f).
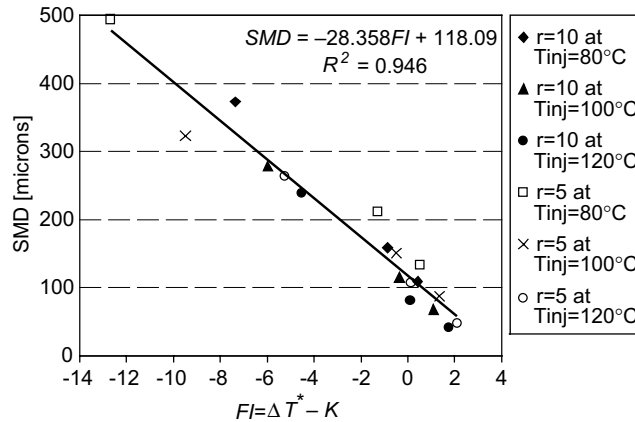
Fig. 19. Correlation for SMD as a function the flushing index, Eqs. (9) and (10).

with an $R^2 = 0.9452$ and standard deviation 30.04 μm. As Fig. 19 shows, this correlation collapses all of the data shown in Figs. 12–17. Eqs. (9) and (10) say that in flash atomization cavitation and superheating are equally important. They are interchangeable in that one can obtain the same SMD through many different combinations of ΔT^* and K. The same SMD can be obtained either under subcooled conditions ($\Delta T^* < 0$) with strong cavitation (low K) or under superheated conditions in the absence of cavitation. Eq. (10) gives a very simple expression for quantifying the interchange between the two mechanisms, thus providing a practical tool for designing flash injectors.

5. Conclusions

The butane–hexadecane binary solution was chosen as a representative model system for studying the influence of cavitation and superheating on flash atomization. Specifically, we addressed the effects of the low boiling *n*-butane as the propellant liquid, propellant gas (nitrogen), and the nozzle internal conditions on *n*-hexadecane atomization. Under appropriately chosen nozzle geometry and operating conditions, the presence of a small amount of *n*-butane can significantly enhance the atomization of *n*-hexadecane. Thus, the flashing (or propellant) liquid can be used to reduce the amount of propellant gas for the same level of atomization. A simple, practical correlation is developed for predicting the SMD as a function of a flushing index which is a measure of the combined effect of cavitation and superheating.

Acknowledgements

References

Allen, W.F., 1951. Flow of a flashing mixture of water and steam through pipes and valves. Trans. AMSE 73, 257–265.

Brennen, C.E., 1995. Cavitation and Bubble Dynamics. Oxford University Press.

Brown, R., York, J.L., 1962. Sprays formed by flashing liquid jets. A.I.Ch.E. J. 8, 149–153.

Gemci, T., Yakut, K., Chigier, N., Ho, T.C., 2001a. Cavitation and flash boiling atomization of water/acetone binary mixtures. In: ILASS-Americas' 2001, Dearborn, MI, 20–23 May 2001, pp. 241–246.

Gemci, T., Yakut, K., Chigier, N., Ho, T.C., 2001b. Cavitation enhanced flash atomization of hydrocarbon liquids. In: ILASS-Europe' 2001, Zurich, Switzerland, 2–6 September 2001.

Gemci, T., Yakut, K., Chigier, N., Ho, T.C., 2004. Flash atomization of water/acetone solutions. Atomization and Sprays. Vol. 4–5.

He, L., Ruiz, F., 1995. Effect of cavitation on flow and turbulence in plain orifices for high-speed atomization. Atomization and Sprays 5, 569–584.

Hitron, R., Chigier, N., Ho, T.C., 1999. Cavitation enhanced atomization at low liquid superheat-conditions. In: ILASS-AMERICAS' 99, Indianapolis, IN, 16–19 May 1999, pp. 225–229.

Ho, T.C., 2003. Property–reactivity correlation for hydrodesulfurization of middle distillates. Appl. Catal., A: General 244, 115–128.

Ho, T.C., Katritzky, A.R., Cato, S., 1992. Effect of nitrogen compounds on cracking catalysts. Ind. Chem. Res. 31, 1589–1597.

Kessler, C., Sloss, C.A., McCahan, S., 1998. Flash atomization in single and binary hydrocarbon sprays. In: ILASS-Americas' 98, Sacramento, CA, 17–20 May 1998, pp. 264–267.

Kline, S.J., McClinctock, F.A., 1953. Describing uncertainties in single-sample experiments. Mech. Eng. 75, 3–8.

Knapp, R.T., Daily, J.W., Hammitt, F.G., 1970. Cavitation. McGraw-Hill.

Kurschat, T.H., Chaves, H., Meier, G.E.A., 1992. Complete adiabatic evaporation of highly superheated liquid jets. J. Fluid Mech. 236, 43–59.

Lefebvre, A.H., 1989. Atomization and Sprays. Hemisphere.

Mansour, A., Chigier, N., Shih, T.I.-P., Kozarek, R.L., 1998. The effect of the hartman cavity on the performance of the USGA nozzle used for aluminum spray forming. Atomization and Sprays 8, 1–24.

Miyatake, O., Tomimura, T., Ide, Y., 1985. Enhancement of spray flash evaporation by means of the injection of bubble nuclei. J. Solar Energy Eng., Trans. ASME 107, 176–182.

Oza, R.D., 1984. On the mechanism of flashing injection of initially subcooled fuels. J. Fluids Eng. 106, 105–109.

Park, B.S., Lee, S.Y., 1994. An experimental investigation of the flash atomization mechanism. Atomization and Sprays 4, 159–179.

Perry, R.H., Green, D., 1984. Perry's Chemical Engineers' Handbook, sixth ed. McGraw-Hill, New York.

Shah, Y.T., Pandit, A.B., Moholkar, V.S., 1999. Cavitation Reaction Engineering. Kluwer Academic/Plenum Publishers, New York.

Sharaf, M., Illman, D.L., Kowalski, B.R., 1986. Chemometrics. John Wiley & Sons, NY.

Sher, E., Zeigerson-Katz, M., 1996. Spray formation by flashing of a binary mixture: an energy balance approach. Atomization and Sprays 6, 447–459.

Tamaki, N., Shimizu, M., Nishida, K., Hiroyasu, H., 1998. Effects of cavitation and internal flow on atomization of a liquid jet. Atomization and Sprays 8, 179–197.

Tamaki, N., Shimizu, M., Hiroyasu, H., 2001. Enhancement of the atomization of a liquid jet by cavitation in a nozzle hole. Atomization and Sprays 11, 125–137.

Veruto, P.B., Habib, E.T., 1979. Fluid Catalytic Cracking with Zeolite Catalysts. Marcel Dekker, New York.

Zeigerson-Katz, M., Sher, E., 1998. Spray formation by flashing of a binary mixture: a parametric study. Atomization and Sprays 8, 255–266.